

# Sustainable development of biomass-derived activated carbon through chemical and physical activations and its effect on the physicochemical and electrochemical activity

*by Rika Taslim*

---

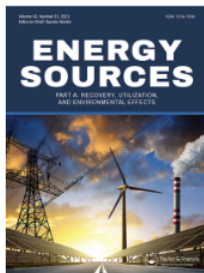
**Submission date:** 12-Apr-2023 01:51PM (UTC+0700)

**Submission ID:** 2062341935

**File name:** 5.\_Coffe\_ENERGY\_SOURCES,\_PART\_A\_2023.pdf (7.16M)

**Word count:** 6514

**Character count:** 33145



## Sustainable development of biomass-derived activated carbon through chemical and physical activations and its effect on the physicochemical and electrochemical activity

Erman Taer, Agustino Agustino, Ester Stefani Gultom & Rika Taslim

To cite this article: Erman Taer, Agustino Agustino, Ester Stefani Gultom & Rika Taslim (2023) Sustainable development of biomass-derived activated carbon through chemical and physical activations and its effect on the physicochemical and electrochemical activity, Energy Sources, Part A: Recovery, Utilization, and Environmental Effects, 45:1, 319-330, DOI: [10.1080/15567036.2023.2168319](https://doi.org/10.1080/15567036.2023.2168319)

To link to this article: <https://doi.org/10.1080/15567036.2023.2168319>



Published online: 19 Jan 2023.



Submit your article to this journal [↗](#)



View related articles [↗](#)



View Crossmark data [↗](#)



# Sustainable development of biomass-derived activated carbon through chemical and physical activations and its effect on the physicochemical and electrochemical activity

Erman Taer<sup>a</sup>, Agustino Agustino<sup>a</sup>, Ester Stefani Gultom<sup>a</sup>, and Rika Taslim<sup>b</sup>

<sup>a</sup>Department of Physics, University of Riau, Simpang Baru, Pekanbaru, Indonesia; <sup>b</sup>Department of Industrial Engineering, State Islamic University of Sultan Syarif Kasim, Simpang Baru, Pekanbaru, Indonesia

## ABSTRACT

Activated carbon derived from biomass waste and their application as supercapacitor electrodes have aroused a considerable research interest in recent years. In this work, we demonstrate the use of *Coffea canephora* leaf (CCL) waste for the preparation of activated carbon as supercapacitor electrodes via chemical activation with straightforward pyrolysis at high temperatures for the first time. Potassium hydroxide with three different concentrations, i.e. 0.1 M, 0.3 M, and 0.5 M, was used as activating agent. The as-prepared activated carbon using 0.3 M KOH (CCL-0.3) displayed good physicochemical properties and exhibited superior electrochemical performance than the other two samples (0.1 and 0.5 M). CCL-0.3 achieved the specific capacitances of 297 F g<sup>-1</sup> and 220 F g<sup>-1</sup> at 1 A g<sup>-1</sup> in 1 M H<sub>2</sub>SO<sub>4</sub> and 1 M Na<sub>2</sub>SO<sub>4</sub> electrolytes, respectively. Moreover, CCL-0.3 in 1 M H<sub>2</sub>SO<sub>4</sub> exhibits the equivalent series resistance ( $R_s$ ) and the charge transfer resistance ( $R_{ct}$ ) value of CCL-0.3 in 1 M H<sub>2</sub>SO<sub>4</sub> of 0.73  $\Omega$  and 4.9  $\Omega$ , respectively. Additionally, this study provides strategies for preparing activated carbon as supercapacitor electrode materials with superior performance via chemical activation with straightforward pyrolysis for the renewable energy storage devices.

## ARTICLE HISTORY

Received 14 June 2022  
Revised 19 December 2022  
Accepted 1 January 2023



## KEYWORDS

*Coffea canephora* leaf; activated carbon; chemical activation and straightforward pyrolysis; electrode materials; supercapacitor

## Introduction

The growing requirement for green, clean, effective, and renewable energy storage equipment has become rising importunate owing to the overuse of fossil fuel consumption and their environmental impact (Wu et al. 2021). To solve these problems, the development of energy storage systems with eco-friendly features and high performance has aroused a tremendous research attention (Wang et al. 2020). In the area of electrochemical energy storage systems, supercapacitors (SCs) or ultracapacitors as backup power sources, advanced energy storage systems, and energy conservation have gained widespread attention over the past few years. SC devices have been employed for various uses, such as electric vehicles, portable electronics, and biomedical equipment.

Owing to their availability, sustainability, renewability, and eco-friendly properties, biomass materials as SC electrodes have become an alternative for meeting the need for sustainable and green carbon sources for further development of SC electrode materials (Amakoromo et al. 2021). For the development of SC electrodes based on biomass waste, much progress has been made in this research field. For example, *Tectona grandis* leaf (Taer et al. 2021) and many biomass wastes including kenaf (Park et al. 2021), sugarcane tip (Wei et al. 2021), green steam of cassava (Taer et al. 2021), bamboo leaf (Jayachandran et al. 2021), *Sapindus trifoliatus* nutshells (Vinayagam et al. 2021), cashew nutshell

**CONTACT** Rika Taslim  [rikataslim@gmail.com](mailto:rikataslim@gmail.com)  Department of Industrial Engineering, State Islamic University of Sultan Syarif Kasim, Simpang Baru, Pekanbaru 28293, Indonesia

© 2023 Taylor & Francis Group, LLC

(Merin et al. 2021), rotten potato (Wang et al. 2021), pecan shell (Zhang et al. 2022), *Allium cepa* peel (Ali et al. 2021), citrus peel fiber (Mondal, Kumar, and Kanti 2021), *Acacia auriculiformis* (Bhat et al. 2021), *Caesalpinia Sappan* (Bhat et al. 2022), and birchwood (popsicle sticks) (Selvaraj et al. 2022) have been employed as alternative carbon sources for SC devices. All of the carbon sources noticed above are inexpensive, sustainable, eco-friendly, and show great performance to be used as SC electrode.

In the present work, we used *Coffea canephora* leaf (CCL) waste as a carbon precursor. Herein, for the first time, we demonstrated the preparation of biomass-derived activated carbon from CCL via KOH activation with straightforward pyrolysis procedures at high temperatures. KOH activation with straightforward pyrolysis and its effect on the physicochemical properties and electrochemical activity of the CCL electrodes were investigated. In addition, the influence of acidic and neutral electrolytes on the electrochemical activity of the sample was also explored. The CCL electrodes were prepared in a free-standing manner without any addition of adhesive material, conductive pigments, etc. More importantly, this study provides an obvious method to select suitable plant waste for sustainable development of biomass-derived activated carbon with superior performance for use as SC electrode materials.

## Material and methods

### Preparation

*Coffea canephora* leaf (CCL) waste was used as raw material for the preparation of activated carbon and was collected from Bengkulu province, Indonesia. First, the leaf was sun-dried for 12 h and then oven-dried for 48 h at 110°C. Afterward, the dried sample was pre-carbonized in at 250°C for 2.5 h and powdered. The powder was mixed into a KOH solution with different concentrations (0.1 M, 0.3 M, and 0.5 M) at 80°C for 2 h; afterward, it was oven-dried for 48 h at 110°C. The dried samples were molded into monolith form under pressure of 8 metrics tons using hydraulic press (Taer and Taslim 2018; Taer et al. 2021, 2021). Then, the monolith forms underwent straightforward pyrolysis via carbonization at 600°C under N<sub>2</sub> gas with subsequent physical activation at 850°C for 2.5 h under CO<sub>2</sub> gas atmosphere. The obtained samples were washed using distilled water until neutral pH was reached. The obtained samples were overnight dried at 110°C and denoted as CCL-0.1, CCL-0.3, and CCL-0.5.

### Material characterization

Scanning electron microscopy (SEM, JEOL-JSM 6510, Japan) along with energy-dispersive X-ray (EDX) was employed to observe the morphology and elemental contents of the CCL samples. The crystal phase structure was detected using X-ray diffraction (XRD, X-pert powder PANalytical) with light source CuK<sub>α</sub> radiation with  $\theta$  ranging between 10 and 80°. The crystal size of the as-prepared samples was obtained using the Debye-Scherrer formula (Ghosh et al. 2019; Jayachandran et al. 2021; Maher et al. 2021). The FT-IR spectrometer (IRprestige A210048, Shimadzu) was applied to explore the functional groups.

### Electrochemical measurements

To evaluate the actual electrochemical performance of the free-standing CCL samples, the symmetrical two-electrode setup was applied and was evaluated in 1 M H<sub>2</sub>SO<sub>4</sub> and 1 M Na<sub>2</sub>SO<sub>4</sub> electrolytes. The free-standing CCL electrodes were used without any adhesive materials, and conductive pigment with a diameter and thickness ranged between  $\pm 0.8$  mm and  $\pm 0.2$  mm were used as a cathode and anode, respectively. The free-standing CCL electrodes were soaked in the electrolyte solution for 48 h. Afterward, the two pieces of electrodes were sandwiched together into a coin cell consisting two stainless steel 316 L plates as current collectors. The cyclic voltammetry (CV) and galvanostatic charge/discharge (GCD) measurements were operated at the potential range of 0–1 V. The

electrochemical impedance spectroscopy (EIS) test was operated at the frequency ranges from 0.01 mHz to 100 kHz. The specific capacitance ( $C_{sp}$ ) based on CV and GCD data was calculated according to Equations (1) and (2):

$$C_{sp} = \frac{2I}{sm} \quad (1)$$

$$C_{sp} = \frac{I\Delta t}{m\Delta V} \quad (2)$$

where  $I$  (A),  $\Delta t$  (s),  $m$  (g),  $\Delta V$  (V) are discharge current, scan rates, total mass of the electrodes, discharge time, and the voltage, respectively. The volumetric capacitance ( $C_v$ ) of the CCL samples was calculated according to the formula:

$$C_v = C_{sp}\rho \quad (3)$$

where  $C_{sp}$  is the specific capacitance ( $F\ g^{-1}$ ) and  $\rho$  is the activated carbon monolith density ( $g\ cm^{-3}$ ). The specific energy ( $E_{sp}$ ) and specific power ( $P_{sp}$ ) were calculated according to Equations (4) and (5), respectively.

$$E_{sp} = \frac{1}{2} C_{sp} V^2 \cdot \frac{1}{3.6} \quad (4)$$

$$P_{sp} = 3600 \frac{E_{sp}}{\Delta t} \quad (5)$$

## Results and discussion

The yields of weight losses after straightforward pyrolysis processes are summarized in Table 1. The straightforward pyrolysis processes accounted for the majority of weight losses. Furthermore, the concentration of KOH is contributed to the carbon yield obtained from the percentage of mass. In the CCL samples, the highest carbon yields were found at 0.1 M KOH concentration (CCL-0.3) whereas there was the lowest carbon yields (CCL-0.1) at 0.3 M KOH concentration. The lower carbon yields on the CCL-0.3 will provide to larger specific surface area and higher porosity (Wang et al. 2021).

The details of morphological structure of CCL samples at 5000 and 40,000 magnifications are represented in Figure 1. Figure 1(a,b) displays the morphological structure of the CCL-0.1 sample. It can be observed that the CCL-0.1 sample is dominated by perforated tunnels which can be linked to volatile gasification during carbonization and activation. The particles showed non-uniformity, whereas the pores also showed different shapes and sizes. Furthermore, it can be seen that the surface morphologies of CCL-0.1 are filled with cavities and are completely irregular as a consequence of the carbonization and activation process with huge amounts of flake and micro-mesopores shaped like slits. It can be known that during the carbonization and activation, the evaporation of  $K_2CO_3$  occurs, resulting in the formation of cavities, leaving empty spaces previously occupied by  $K_2CO_3$  (Mai et al. 2019). A substantial change in morphology is seen on the CCL-0.3 sample as a result of change in KOH concentration and is displayed in Figure 1(c,d). As presented in Figure 1(c), it can be observed that the surface structure of CCL-0.3 is dominated by fine particles with a rod-like structure. However,

**Table 1.** The percentage of weight losses, and carbon yields of CCL samples.

Samples	Weight losses (%)	Carbon yields (%)
CCL-0.1	72.27	27.73
CCL-0.3	84.74	15.26
CCL-0.5	77.35	22.65

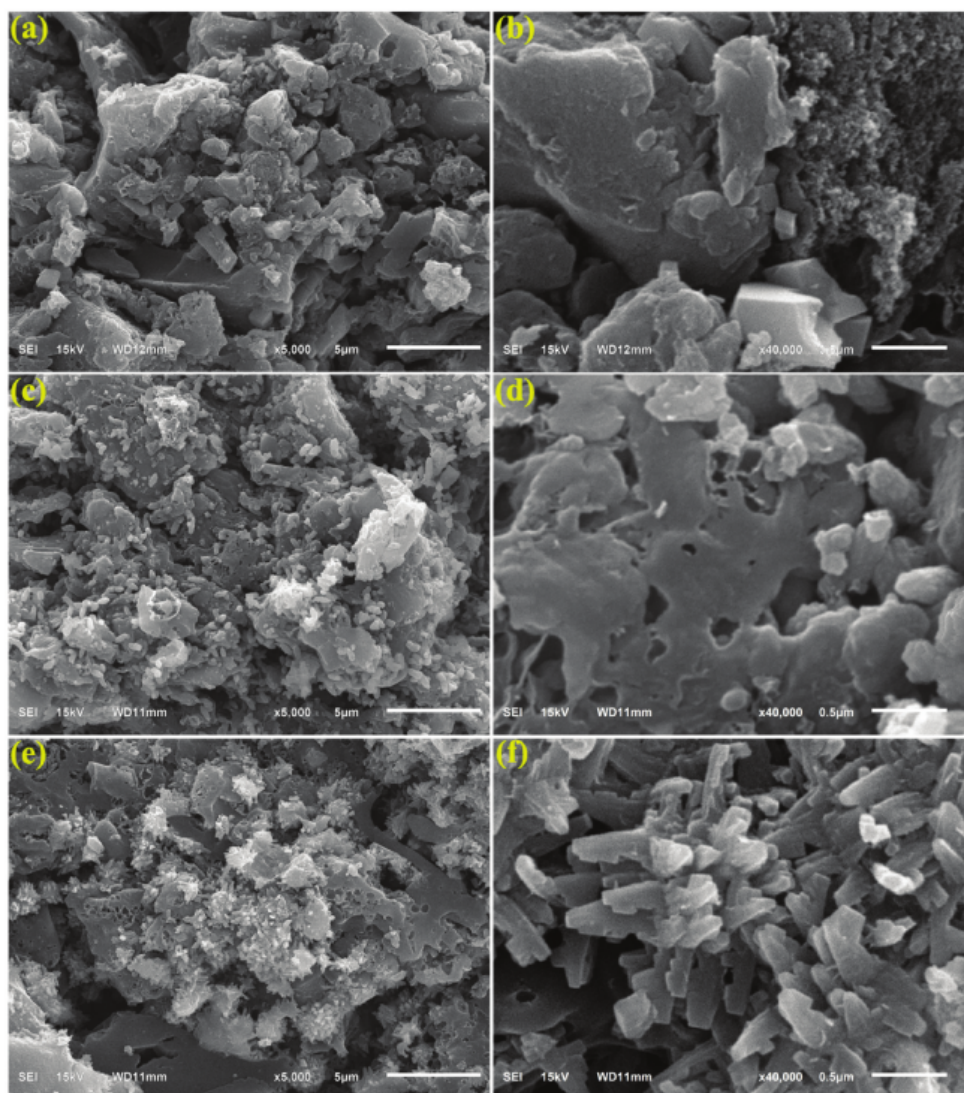


**Figure 1.** SEM image of CCL-0.1 (a and b), CCL-0.3 (c and d), and CCL-0.5 (e and f) at different magnifications.

at the higher magnification (see [Figure 1\(d\)](#)), the presence of hollow pore structures on the surface of sample can be seen. These changes in morphological on the CCL-0.3 can be attributed to the removal of volatile components from the *Coffea canephora* leaf through the decomposition of lignocellulosic. During the carbonization and activation process, the moisture from the lignin is evaporated, and the inorganic component produces volatile undergoes decomposition, resulting in the porous network. Extreme changes in the surface structure of the CCL sample are also seen at CCL-0.5 and depicted in [Figure 1\(e,f\)](#). As represented in [Figure 1\(e\)](#), it can be observed that the surface structure of CCL-0.5 consists of a large amount of fine particles with crystal-like shape and the figure also shows the presence of hollow pores on the surface of CCL-0.5. Furthermore, at the higher magnification (see [Figure 1\(F\)](#)), surface structure of CCL-0.5 shows the sheet-like structure jagged of various sizes. These structure are most likely the calcium compounds as shown by the EDS results (see [Table 1](#)) which has high calcium content in the CCL-0.1 sample (6.38 wt%).

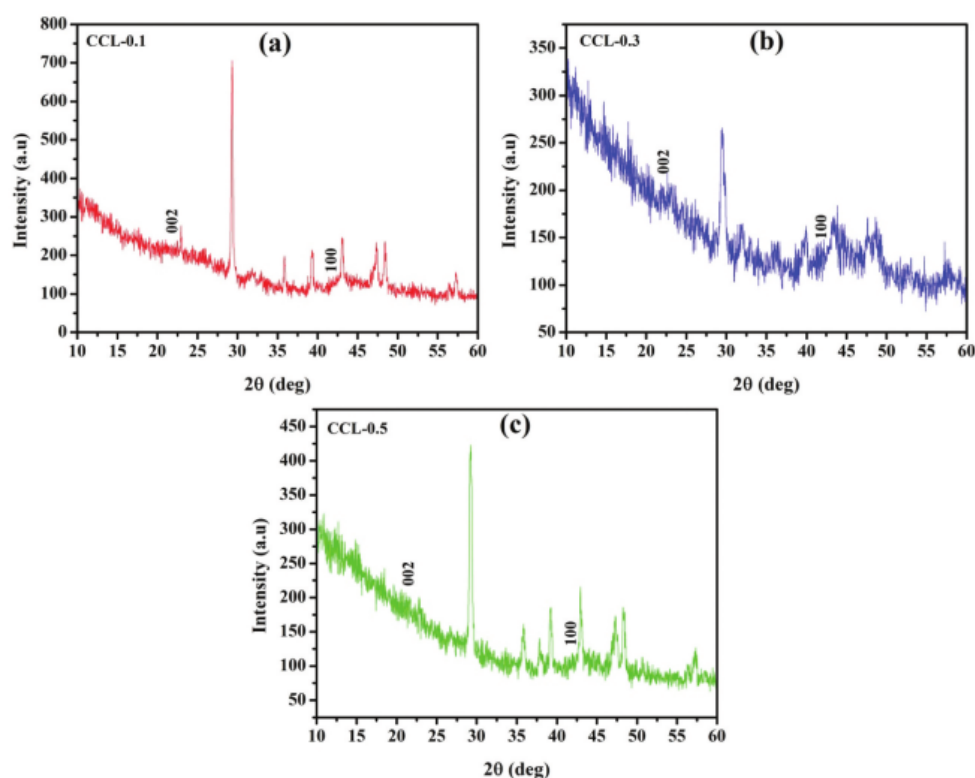
[Table 2](#) shows the EDS results of the CCL-0.1, CCL-0.3, and CCL-0.5 samples. All three samples clearly show the existence of carbon, oxygen, magnesium, calcium, and niobium, but the EDS spectra

**Table 2.** EDS results of the CCL samples.

Samples	Elements					
	C(% wt)	O(% wt)	Na(% wt)	Mg(% wt)	Ca(% wt)	Nb(% wt)
0.1 M	77.95	14.15	-	0.7	5.00	2.20
0.3 M	72.75	18.91	0.05	0.61	5.55	2.13
0.5 M	73.92	17.02	-	0.79	6.38	1.89

of the CCL-0.3 sample show the presence of the element sodium. All the CCL samples are dominated by the carbon and oxygen contents with >70 wt% and >17 wt%, respectively. The CCL-0.3 showed a higher oxygen content than the CCL-0.1 and CCL-0.5. It can be inferred that the CCL-0.3 has a good electrochemical performance. The other elements, i.e. sodium, calcium, magnesium, and niobium, most likely are inorganic elements which are naturally present in the raw materials.

To identify the crystal phase structure of the CCL samples, the XRD spectra of CCL-0.1, CCL-0.3, and CCL-0.5 are displayed in Figure 2. The primary diffraction peaks of activated carbon can be identified by the XRD spectra, which demonstrate the characteristic of amorphous features of the carbonaceous material. Two prevalent diffraction peaks at  $2\theta$  around  $22\text{--}24^\circ$  and  $42\text{--}44^\circ$  can be associated with the (002) and (100) crystal planes, respectively (Lu et al. 2018; Ma et al. 2018). Generally, in the XRD spectra of CCL-0.1, CCL-0.3, and CCL-0.5, relatively there is no difference, indicating that no graphitization occurred the increasing KOH concentration during chemical activation process. Moreover, the obtained sharp peaks of CCL-0.1, CCL-0.3, and CCL-0.5 positioned at  $2\theta$  indicated the presence of silica oxide ( $\text{SiO}_2$ ) in the samples. The sharp peaks were reduced upon the increase of KOH concentration from 0.1 M to 0.3 M that leads to the decline of crystallinity; inversely, by increasing the concentration of KOH to 0.5 M, the sharp peaks were increased on the CCL-0.5.

**Figure 2.** XRD spectra of CCL-0.1 (a), CCL-0.3 (b), and CCL-0.5 (c).

From Scherer's formula, the crystallite size of the CCL samples was obtained and shows a considerable change following the concentration of KOH. It occurs around of 0.513 nm for CCL-0.1, while it drops to 0.415 nm for CCL-0.3. While the rise of concentration into 0.5 M induced the rise of crystallite size to be 0.504 nm for CCL-0.5. The effect of KOH concentration changes toward susceptibility of regularity via lattice stacking refers to the orientation of crystallographic differentiation. The calculated of interlayer distance value ( $d_{002}$ ), the CLs samples have the higher value than graphite (3.35 Å). The CCL-0.3 has the lowest interlayer distance with 3.56 Å, whereas CCL-0.1 and CCL-0.5 have 4.07 Å and 3.67 Å, respectively.

The FTIR spectra of CCL-0.1, CCL-0.3, and CCL-0.5 are represented in Figure 3. The bands are observed at  $3454.29\text{ cm}^{-1}$ ,  $3464.01\text{ cm}^{-1}$ , and  $3473.12\text{ cm}^{-1}$  which correspond to the O-H group's (carboxyl acid) stretching vibrations. The C=C stretching vibration was observed at  $1632.62\text{ cm}^{-1}$ ,  $1645.56\text{ cm}^{-1}$  and  $1626.93\text{ cm}^{-1}$ . Furthermore, the peaks at  $1121.10\text{ cm}^{-1}$ ,  $1120.68\text{ cm}^{-1}$ , and  $1110.96\text{ cm}^{-1}$  are attributed to the existence of C-O stretching vibration.

### Electrochemical activity analysis

To explore the performance of the different free-standing CCL electrodes in  $1\text{ M H}_2\text{SO}_4$  and  $1\text{ M Na}_2\text{SO}_4$  electrolytes, cyclic voltammetry was used and applied in symmetrical two-electrode setup and are displayed in Figure 4(a,b). The CV profile of the CCL electrodes in both electrolytes has a mechanism of storage based on the creation of charge-separated state in the electric double layer before and generally have a quasi-rectangular-shaped characteristics. The larger CV area of CCL-0.3 in  $1\text{ M H}_2\text{SO}_4$  and  $1\text{ M Na}_2\text{SO}_4$  electrolytes can be observed from Figure 4(a,b), indicating that it had a higher capacitance than CCL-0.1 and CCL-0.5. The value of specific capacitances of CCL-0.1, CCL-0.3, and CCL-0.5 at  $1\text{ mV s}^{-1}$  was obtained to be  $129\text{ F g}^{-1}$ ,  $177\text{ F g}^{-1}$ , and  $139\text{ F g}^{-1}$  for  $\text{H}_2\text{SO}_4$  electrolyte,  $59\text{ F g}^{-1}$ ,  $130\text{ F g}^{-1}$ , and  $99\text{ F g}^{-1}$  for  $\text{Na}_2\text{SO}_4$  electrolyte, respectively.

Figure 4(c,d) displays the influence on the specific capacitances with the rise in scan rate for all the CCL samples in  $1\text{ M H}_2\text{SO}_4$  and  $1\text{ M Na}_2\text{SO}_4$  electrolytes, respectively. It was can be observed that CCL-0.3 possess a higher specific capacitance compared to CCL-0.1 and CCL-0.5 in both electrolytes. Moreover, as seen from Figures 4(c,d), the specific capacitance declines with rises in scan rates and vice versa. This is owing to the insufficient use of dynamic electrode active sites by ion of electrolytes with rise in scan rates (Ahmed, Ahmed, and Rafat 2018; Ahmed and Rafat 2018). Furthermore, it can be concluded that CCLs in  $1\text{ M H}_2\text{SO}_4$  have a higher specific capacitance value

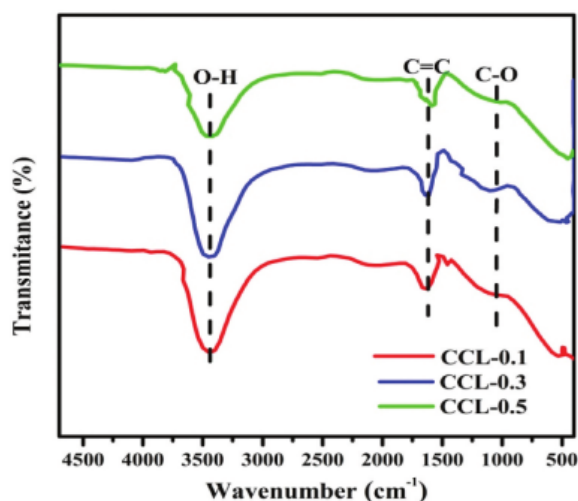
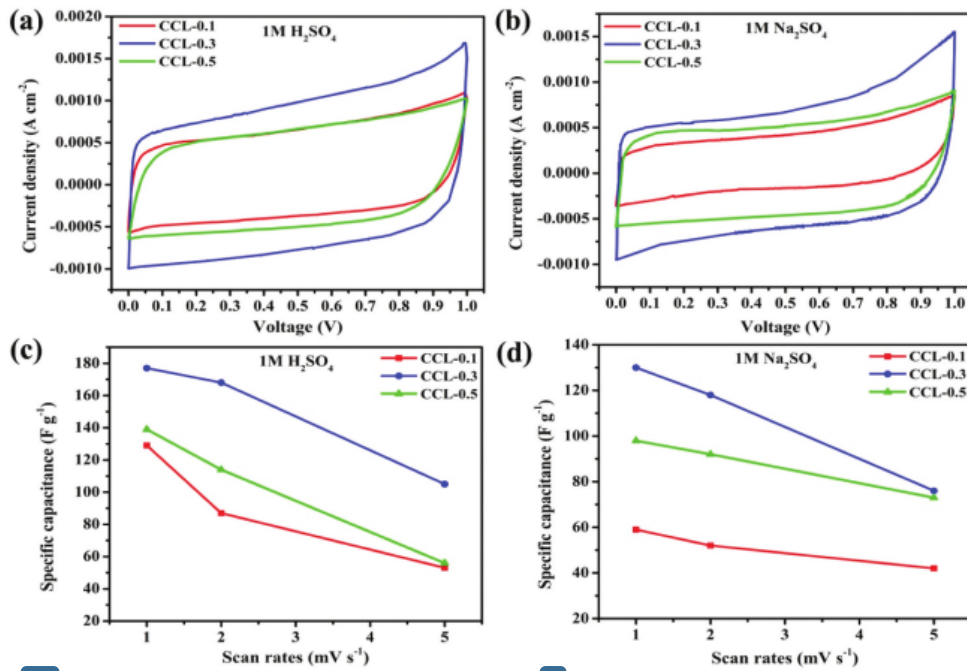


Figure 3. FTIR spectra of CCL-0.1, CCL-0.3, and CCL-0.5.





**Figure 4.** CV curve of the CCL samples (a) in 1 M H<sub>2</sub>SO<sub>4</sub> electrolyte, (b) in 1 M Na<sub>2</sub>SO<sub>4</sub> electrolyte, and specific capacitance vs. scan rates of the CCL samples, (c) in 1 M H<sub>2</sub>SO<sub>4</sub> electrolyte, and (d) in 1 M Na<sub>2</sub>SO<sub>4</sub> electrolyte.

than the CCLs in 1 M Na<sub>2</sub>SO<sub>4</sub> electrolyte. The specific capacitance of the CCL samples in 1 M H<sub>2</sub>SO<sub>4</sub> and 1 M Na<sub>2</sub>SO<sub>4</sub> electrolytes at different scan rates are mentioned in Table 3.

In order to estimate the specific capacitance of supercapacitors, the GCD study is a trustful and practical method. The GCD studies are shown for the free-standing CCL electrodes in different aqueous electrolytes and are presented in Figure 5. Figures 5(a,b) display the GCD curves of CCL-0.1, CCL-0.3, and CCL-0.5 at 1 A g<sup>-1</sup> in 1 M H<sub>2</sub>SO<sub>4</sub> and 1 M Na<sub>2</sub>SO<sub>4</sub> electrolytes, respectively. The GCD curves for all the CCL electrodes show a nearly triangular shape, demonstrating a good electrochemical stability and good ion accessibility at the interface of electrode/electrolyte, indicating the charge storage mechanism of the CCL electrodes. The specific capacitance of CCL-0.1, CCL-0.3, and CCL-0.5 were found to be 128 F g<sup>-1</sup>, 297 F g<sup>-1</sup> and 207 F g<sup>-1</sup> for H<sub>2</sub>SO<sub>4</sub> electrolyte, 67 F g<sup>-1</sup>, 220 F g<sup>-1</sup> and 191 F g<sup>-1</sup> for Na<sub>2</sub>SO<sub>4</sub> electrolyte, respectively. Furthermore, the calculated volumetric capacitance of CCL-0.1, CCL-0.3, and CCL-0.5 are 13.63 F cm<sup>-3</sup>, 20.99 F cm<sup>-3</sup>, and 20.40 F cm<sup>-3</sup> for H<sub>2</sub>SO<sub>4</sub> electrolyte, 7.13 F cm<sup>-3</sup>, 15.55 F cm<sup>-3</sup>, and 18.82 F cm<sup>-3</sup> for Na<sub>2</sub>SO<sub>4</sub> electrolyte, respectively. In both electrolyte solutions, the CCL-0.3 electrode demonstrates higher specific capacitances than the CCL-0.1 and CCL-0.5 electrodes. The higher specific capacitance of CCL-0.3 can be attributed to the higher oxygen content in the sample, as confirmed by the EDS result. In addition, the CCL-0.3 electrode in H<sub>2</sub>SO<sub>4</sub> has a better interaction with the H<sub>2</sub>SO<sub>4</sub> ions than the Na<sub>2</sub>SO<sub>4</sub> ions. It can be decided that the penetration of H<sub>2</sub>SO<sub>4</sub> ions to the inner pore of CCL-0.3 is much easier during the process of charge/discharge. The

**Table 3.** The specific capacitance of the CCL samples in 1 M H<sub>2</sub>SO<sub>4</sub> and 1 M Na<sub>2</sub>SO<sub>4</sub> electrolytes at different scan rates.

Scan rates (mV s <sup>-1</sup> )	C <sub>sp</sub> (F g <sup>-1</sup> ) in H <sub>2</sub> SO <sub>4</sub>			C <sub>sp</sub> (F g <sup>-1</sup> ) in Na <sub>2</sub> SO <sub>4</sub>		
	CCL-0.1	CCL-0.3	CCL-0.5	CCL-0.1	CCL-0.3	CCL-0.5
1	129	177	139	59	130	98
2	87	168	114	52	118	92
5	53	105	56	42	76	73

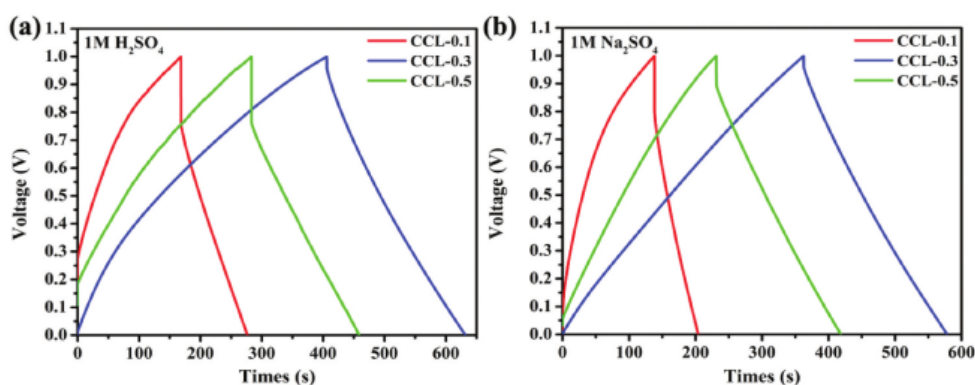


Figure 5. GCD curves of the CCL sample (a) in  $\text{H}_2\text{SO}_4$  electrolyte and (b) in  $\text{Na}_2\text{SO}_4$  electrolyte.

different hydrated radius, ionic mobility, and molar ionic conductivity in  $\text{H}_2\text{SO}_4$  and  $\text{Na}_2\text{SO}_4$  electrolytes also affected the performance of CCL-0.3.

The specific energy and specific power of the CCL samples are calculated by Equations (4) and (5). The maximum specific energy for the CCL samples is obtained on the CCL-0.3 sample for both electrolyte solutions. The specific energy of the CCL-0.3 samples is  $41.25 \text{ Wh kg}^{-1}$  at specific power of  $657.95 \text{ W kg}^{-1}$  in  $1 \text{ M H}_2\text{SO}_4$ ,  $30.56 \text{ Wh kg}^{-1}$  at specific power of  $510.28 \text{ W kg}^{-1}$  in  $1 \text{ M Na}_2\text{SO}_4$ . This value is significantly larger than the most previously reported electrode materials prepared from other biomass precursors such as kelp, water chestnut, mango seed, black tea, and pineapple leaf fibers, and are summarized in Table 4.

To estimate the conception of the interactions of between electrode/electrolyte, the EIS measurement is required to represent Nyquist plots of the CCL-0.3 electrode. The Nyquist plot ( $-Z''$  vs  $Z'$  plot) at varying frequencies of CCL-0.3 in  $1 \text{ M H}_2\text{SO}_4$  is shown in Figure 6(a). Figure 6(a) displays a Nyquist curve of CCL-0.3 using Corrtest Studio v6.0 software. In the high-frequency region, the Nyquist curve shows a semicircle, while in the low-frequency region, it shows a vertical line to demonstrate the resistance of

Table 4. Electrochemical performance of the CCL samples compared to other biomass precursors previously reported.

Carbon precursor	Electrolytes	$C_{sp}$ ( $\text{F g}^{-1}$ )	$E_{sp}$ ( $\text{Wh kg}^{-1}$ )	$P_{sp}$ ( $\text{W kg}^{-1}$ )	References
<i>Tectona grandis</i> leaf	$1 \text{ M H}_2\text{SO}_4$	168	23.19	83.56	(Taer et al. 2021)
Kenaf	$6 \text{ M KOH}$	212	6	215	(Park et al. 2021)
Sugarcane tip	$6 \text{ M KOH}$	228.3	7.93	100	(Wei et al. 2021)
<i>Sapindus trifoliatus</i> nut shells	$6 \text{ M KOH}$	240.8	30	400	(Vinayagam et al. 2021)
Pineapple leaf fiber	$1 \text{ M H}_2\text{SO}_4$	133	27	148	(Kongthong et al. 2022)
Teak leaves	$1 \text{ M H}_2\text{SO}_4$	280	9.72	70.12	(Taer et al. 2021)
<i>Terminalia cattapa</i> leaf	$1 \text{ M H}_2\text{SO}_4$	54	-	-	(Taer et al. 2018)
Tobacco waste	$6 \text{ M KOH}$	120	2.66	51	(Chen et al. 2017)
Cotton	$6 \text{ M KOH}$	270	18	250	(Zhang et al. 2018)
Cottonseed hull waste	$6 \text{ M KOH}$	346	-	-	(Jiang et al. 2020)
Cellulose carbamate	$6 \text{ M KOH}$	289	-	-	(Zhou et al. 2017)
Cottonseed hull	$6 \text{ M KOH}$	304	21.1	250	(Jiang et al. 2018)
Kelp	$6 \text{ M KOH}$	166	5.76	124.92	(Li et al. 2021)
Mango seeds	$2 \text{ M NaOH}$	135	19	1077	(Wickramaarachchi et al. 2021)
Black tea	$6 \text{ M KOH}$	482.1	19.1	325	(Zhang et al. 2021)
Wheat straw and food waste	$6 \text{ M KOH}$	81.6	11.3	240	(Liu et al. 2021)
Native European deciduous trees	$1 \text{ M H}_2\text{SO}_4$	24	0.53	51	(Jain et al. 2021)
Water chestnut shell	$6 \text{ M KOH}$	318	-	-	(Ma et al. 2022)
Zirconia-based carbon nanofiber	$6 \text{ M KOH}$	140	4.86	250	(Aydın et al. 2022)
<i>Hibiscus sabdariffa</i> fruits	$0.5 \text{ M Na}_2\text{SO}_4$	29	13.10	225	(Hamouda et al. 2020)
Pinecone	$1 \text{ M H}_2\text{SO}_4$	43	5.97	253	(Rajesh et al. 2020)
<i>Coffea canephora</i> leaf	$1 \text{ M H}_2\text{SO}_4$	297	41.25	657.95	This work
	$1 \text{ M Na}_2\text{SO}_4$	220	30.56	510.28	

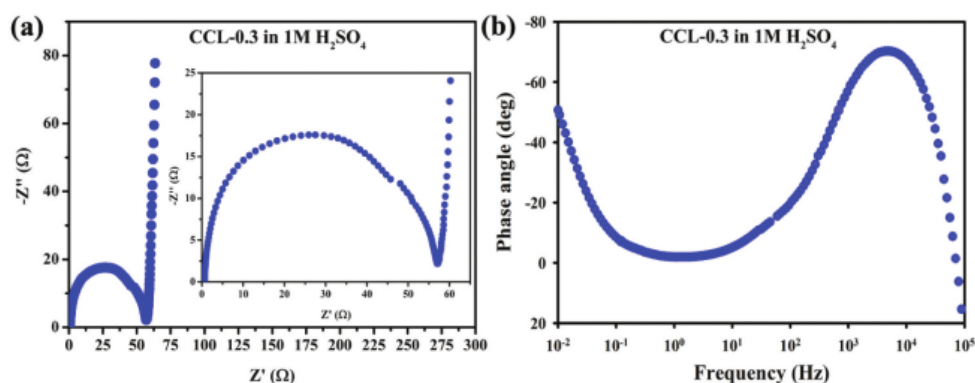


Figure 6. (a) Nyquist plot and (b) Bode phase angle plot (deg) vs. frequency (Hz) of CCL-0.3 in 1 M  $\text{H}_2\text{SO}_4$ .

charge transfer in the electrolyte ions and diffusion of them in the pore of electrodes. In particular, an increase of Warburg tails with slopes close to  $90^\circ$  at low frequencies demonstrates that the activated carbon 5 especially CCL-0.3, possesses perfectly EDLC characteristic (Senthilkumar et al. 2013; Wan et al. 2019). The equivalent series resistance ( $R_s$ ) and the charge transfer resistance ( $R_{ct}$ ) values of CCL-0.3 in 1 M  $\text{H}_2\text{SO}_4$  are  $0.73 \Omega$  and  $4.9 \Omega$ , respectively. Figure 6(b) depicts the phase angle (degree) vs. response frequency (Hz) of CCL-0.3 in 1 M  $\text{H}_2\text{SO}_4$ . Based on the Bode phase angle plot, it was clear that CCL-0.3 in 1 M  $\text{H}_2\text{SO}_4$  has phase angle at  $-50.66^\circ$  at a low frequency, around 0.01 Hz, which further confirmed the charge storage feature of double layer (Sankar and Kalai Selvan 2015; Senthilkumar et al. 2013).

## Conclusions

In summary, *Coffea canephora* leaf has been successfully prepared via chemical activation with straightforward pyrolysis procedures for the first time. KOH with different concentrations, i.e. 0.1 M, 0.3 M, and 0.5 M, were used as an activator for the chemical activation. The sample prepared using 0.3 M KOH (CCL-0.3) displayed a good physicochemical properties and exhibited a superior electrochemical performance as SC electrode materials compared to the other two samples (0.1 and 0.5 M). The symmetrical device prepared using CCL-0.3 as anode and cathode electrodes showed a superior electrochemical performance with specific capacitances of  $297 \text{ F g}^{-1}$  in 1 M  $\text{H}_2\text{SO}_4$  19 and  $220 \text{ F g}^{-1}$  in 1 M  $\text{Na}_2\text{SO}_4$  electrolytes, respectively. Furthermore, the CCL-0.3 has a maximum specific energy of  $41.25 \text{ Wh kg}^{-1}$  at specific power of  $657.95 \text{ W kg}^{-1}$  in 1 M  $\text{H}_2\text{SO}_4$ ,  $30.56 \text{ Wh kg}^{-1}$  at specific power of 43.28  $\text{W kg}^{-1}$  in 1 M  $\text{Na}_2\text{SO}_4$ , respectively. Furthermore, the CCL-0.3 electrode in 1 M  $\text{H}_2\text{SO}_4$  has the  $R_s$  and  $R_{ct}$  values of  $0.73 \Omega$  and  $4.9 \Omega$ , respectively. This study confirmed that biomass-derived activated carbon prepared from the *Coffea canephora* leaf via KOH activation with straightforward pyrolysis procedures at high temperatures shows to be a promising candidate for electrode materials for the development of SC devices.

13

## Acknowledgements

This research was financially supported by the Kementerian Pendidikan, Kebudayaan, Riset, dan Teknologi, Republic of Indonesia via the second year of the WCR grant (Contract no. 1627/UN19.5.1.3/PT.01.03/2022) and the LPPM 48 Islamic University of Sultan Syarif Kasim via the Collaboration Cluster Research Grants between Universities (contract no. 873/Un.04/L.1/TL.01/03/2022).

6

## Disclosure statement

No potential conflict of interest was reported by the authors.

## Funding

The work was supported by the Ministry of Education and Culture LPPM Universitas Islam Negeri Sultan Syarif Kasim [873/Un.04/L.1/TL.01/03/2022].

## References

- Ahmed, S., A. Ahmed, and M. Rafat. 2018. Supercapacitor performance of activated carbon derived from rotten carrot in aqueous, organic and ionic liquid based electrolytes. *Journal of Saudi Chemical Society* 22 (8):993–1002. doi:10.1016/j.jscs.2018.03.002.
- Ahmed, S., and M. Rafat. 2018. Hydrothermal synthesis of PEDOT/rGO composite for supercapacitor applications. *Materials Research Express* 5 (1):015507. doi:10.1088/2053-1591/aaa232.
- Ali, G. A. M., S. Supriya, K. F. Chong, E. R. Shaaban, H. Algarni, T. Maiyalagan, and G. Hegde. 2021. Superior supercapacitance behavior of oxygen self-doped carbon nanospheres: A conversion of Allium cepa peel to energy storage system. *Biomass Conversion and Biorefinery* 11 (4):1311–23. doi:10.1007/s13399-019-00520-3.
- Amakoromo, T. E., O. E. Abumere, J. A. Amusan, V. Anye, and A. Bello. 2021. Porous carbon from Manihot Esculenta (cassava) peels waste for charge storage applications. *Current Research in Green and Sustainable Chemistry* 4 (February):100098. doi:10.1016/j.crgsc.2021.100098.
- Aydn, H., U. Kurtan, M. Demir, and S. Karakuş. 2022. Synthesis and application of a self-standing zirconia-based carbon nanofiber in a supercapacitor. *Energy & Fuels* 36 (4):2212–19. doi:10.1021/acs.energyfuels.1c04208.
- Bhat, V. S., T. Arafat, G. Hegde, and R. S. Varma (2022). Capacitive dominated charge storage in supermicropores of self-activated carbon electrodes for symmetric supercapacitors. *Journal of Energy Storage*, 52, Part A (1 August 2022), 104776. doi:10.1016/j.est.2022.104776
- Bhat, V. S., T. J. Jayeoye, T. Rujiralai, U. Sirimahachai, K. F. Chong, and G. Hegde. 2021. Acacia auriculiformis – derived bimodal porous nanocarbons via self-activation for high-performance supercapacitors. *Frontiers in Energy Research* 9 (September):1–15. doi:10.3389/fenrg.2021.744133.
- Chen, H., Y. C. Guo, F. Wang, G. Wang, P. R. Qi, X. H. Guo, B. Dai, and F. Yu. 2017. An activated carbon derived from tobacco waste for use as a supercapacitor electrode material. *New Carbon Materials* 32 (6):592–99. doi:10.1016/S1872-5805(17)60140-9.
- Ghosh, S., R. Santhosh, S. Jeniffer, V. Raghavan, G. Jacob, K. Nanaji, P. Kollu, S. K. Jeong, and A. N. Grace. 2019. Natural biomass derived hard carbon and activated carbons as electrochemical supercapacitor electrodes. *Scientific Reports* 9 (1):1–15. doi:10.1038/s41598-019-52006-x.
- Hamouda, H. A., S. Cui, X. Dai, L. Xiao, X. Xie, H. Peng, and G. Ma. 2020. Synthesis of porous carbon material based on biomass derived from hibiscus sabdariffa fruits as active electrodes for high-performance symmetric supercapacitors. *RSC advances* 11 (1):354–63. doi:10.1039/d0ra09509e.
- Jain, A., M. Ghosh, M. Krajewski, S. Kurungot, and M. Michalska. 2021. Biomass-derived activated carbon material from native European deciduous trees as an inexpensive and sustainable energy material for supercapacitor application. *Journal of Energy Storage* 34 (September 2020):102178. doi:10.1016/j.est.2020.102178.
- Jayachandran, M., S. Kishore Babu, T. Maiyalagan, N. Rajadurai, and T. Vijayakumar. 2021. Activated carbon derived from bamboo-leaf with effect of various aqueous electrolytes as electrode material for supercapacitor applications. *Materials letters* 301 (June):130335. doi:10.1016/j.matlet.2021.130335.
- Jayachandran, M., A. Rose, T. Maiyalagan, N. Poongodi, and T. Vijayakumar. 2021. Effect of various aqueous electrolytes on the electrochemical performance of  $\alpha$ -MnO<sub>2</sub> nanorods as electrode materials for supercapacitor application. *Electrochimica acta* 366:137412. doi:10.1016/j.electacta.2020.137412.
- Jiang, Y., Y. Liu, Y. Zhang, Y. Chen, and X. Zan. 2020. Micro-structure determines the intrinsic property difference of bio-based nitrogen-doped porous carbon—a case study. *Nanomaterials* 10 (9):1765. doi:10.3390/nano10091765.
- Jiang, Y., Z. Zhang, Y. Zhang, X. Zhou, L. Wang, A. Yasin, and L. Zhang. 2018. Bioresource derived porous carbon from cottonseed hull for removal of triclosan and electrochemical application †. *RSC advances* 8 (74):42405–14. doi:10.1039/c8ra08332k.
- Kongthong, T., C. Poochai, C. Sriprachubwong, A. Tuantranont, S. Nanan, N. Meethong, P. Pakawatpanurut, T. Amornsakchai, and J. Sotipinta. 2022. Microwave-assisted synthesis of nitrogen-doped pineapple leaf fiber-derived activated carbon with manganese dioxide nanofibers for high-performance coin- and pouch-cell supercapacitors. *Journal of Science: Advanced Materials and Devices* 7 (2):100434. doi:10.1016/j.jsamd.2022.100434.
- Li, L., X. Hu, N. Guo, S. Chen, Y. Yu, and C. Yang. 2021. Synthesis O/S/N doped hierarchical porous carbons from kelp via two-step carbonization for high rate performance supercapacitor. *Journal of Materials Research and Technology* 15:6918–28. doi:10.1016/j.jmrt.2021.11.076.
- Liu, Z., J. Hu, F. Shen, D. Tian, M. Huang, J. He, J. Zou, L. Zhao, and Y. Zeng. 2021. Trichoderma bridges waste biomass and ultra-high specific surface area carbon to achieve a high-performance supercapacitor. *Journal of Power Sources* 497 (January):229880. doi:10.1016/j.jpowsour.2021.229880.

- Lu, C., Y. H. Huang, Y. J. Wu, J. Li, and J. P. Cheng. 2018. Camellia pollen-derived carbon for supercapacitor electrode material. *Journal of Power Sources* 394 (May):9–16. doi:10.1016/j.jpowsour.2018.05.032.
- Ma, C., J. Bai, M. Demir, X. Hu, S. Liu, and L. Wang. 2022. Water chestnut shell-derived N/S-doped porous carbons and their applications in CO<sub>2</sub> adsorption and supercapacitor. *Fuel* 326:125119. doi:10.1016/j.fuel.2022.125119.
- Ma, C., E. Cao, J. Li, Q. Fan, L. Wu, Y. Song, and J. Shi. 2018. Synthesis of mesoporous ribbon-shaped graphitic carbon nanofibers with superior performance as efficient supercapacitor electrodes. *Electrochimica acta* 292:364–73. doi:10.1016/j.electacta.2018.07.135.
- Maher, M., S. Hassan, K. Shouair, B. Yousif, and M. E. A. Abo-Elhoud. 2021. Activated carbon electrode with promising specific capacitance based on potassium bromide redox additive electrolyte for supercapacitor application. *Journal of Materials Research and Technology* 11:1232–44. doi:10.1016/j.jmrt.2021.01.080.
- Mai, T. T., D. L. Vu, D. C. Huynh, N. L. Wu, and A. T. Le. 2019. Cost-effective porous carbon materials synthesized by carbonizing rice husk and K<sub>2</sub>CO<sub>3</sub> activation and their application for lithium-sulfur batteries. *Journal of Science: Advanced Materials and Devices* 4 (2):223–29. doi:10.1016/j.jsamd.2019.04.009.
- Merin, P., P. Jimmy Joy, M. N. Muralidharan, E. Veena Gopalan, and A. Seema. 2021. Biomass-derived activated carbon for high-performance supercapacitor electrode applications. *Chemical Engineering & Technology* 44 (5):844–51. doi:10.1002/ceat.202000450.
- Mondal, M., D. Kumar, and T. Kanti. 2021. Lignocellulose based bio-waste materials derived activated porous carbon as superior electrode materials for high-performance supercapacitor. *Journal of Energy Storage* 34 (December 2020):102229. doi:10.1016/j.est.2020.102229.
- Park, H. Y., M. Huang, T. -H. Yoon, and K. H. Song. 2021. Electrochemical properties of kenaf-based activated carbon monolith for supercapacitor electrode applications. *RSC advances* 11 (61):38515–22. doi:10.1039/d1ra07815a.
- Rajesh, M., R. Manikandan, S. Park, B. C. Kim, W. J. Cho, K. H. Yu, and C. J. Raj. 2020. Pinecone biomass-derived activated carbon: The potential electrode material for the development of symmetric and asymmetric supercapacitors. *International Journal of Energy Research* 44 (11):8591–605. doi:10.1002/er.5548.
- Sankar, K. V., and R. Kalai Selvan. 2015. Improved electrochemical performances of reduced graphene oxide based supercapacitor using redox additive electrolyte. *Carbon* 90:260–73. doi:10.1016/j.carbon.2015.04.023.
- Selvaraj, A. R., D. Chinnadurai, I. Cho, J. -S. Bak, and K. Prabakar. 2022. Bio-waste wood-derived porous activated carbon with tuned microporosity for high performance supercapacitors. *Journal of Energy Storage* 52 Part B(15 August 2022):104928. doi:10.1016/j.est.2022.104928.
- Senthilkumar, S. T., R. K. Selvan, Y. S. Lee, and J. S. Melo. 2013. Electric double layer capacitor and its improved specific capacitance using redox additive electrolyte. *Journal of Materials Chemistry A* 1 (4):1086–95. doi:10.1039/c2ta00210h.
- Taer, E., A. Afrianda, R. Taslim, K. Krisman, M. Minarni, A. Agustino, A. Apriwandi, and U. Malik. 2018. The physical and electrochemical properties of activated carbon electrode made from Terminalia Catappa leaf (TCL) for supercapacitor cell application. *Journal of Physics Conference Series* 1120 (1):012007. doi:10.1088/1742-6596/1120/1/012007.
- Taer, E., M. A. Mardiah, A. Agustino, W. S. Mustika, A. Apriwandi, and R. Taslim. 2021. A green and low-cost of mesoporous electrode based activated carbon monolith derived from fallen teak leaves for high electrochemical performance. *Journal of Applied Engineering Science* 19 (1):162–71. doi:10.5937/jaes0-27589.
- Taer, E., M. Melisa, A. Agustino, R. Taslim, W. Sinta, and A. Apriwandi. 2021. Biomass-based activated carbon monolith from Tectona grandis leaf as supercapacitor electrode materials. *Energy Sources, Part A: Recovery, Utilization, and Environmental Effects* 00 (00):1–12. doi:10.1080/15567036.2021.1950871.
- Taer, E., and R. Taslim (2018). Brief review: Preparation techniques of biomass based activated carbon monolith electrode for supercapacitor applications. *AIP Conference Proceedings, 1927*. doi:10.1063/1.5021192
- Taer, E., N. Yanti, W. S. Mustika, A. Apriwandi, R. Taslim, and A. Agustino. 2021. Porous activated carbon monolith with nanosheet/nanofiber structure derived from the green stem of cassava for supercapacitor application. *International Journal of Energy Research* 44 (13):10192–205. doi:10.1002/er.5639.
- Vinayagam, M., R. Suresh Babu, A. Sivasamy, and A. L. F. de Barros. 2021. Biomass-derived porous activated carbon nanofibers from Sapindus trifoliatus nut shells for high-performance symmetric supercapacitor applications. *Carbon Letters* 31 (6):1133–43. doi:10.1007/s42823-021-00235-4.
- Wang, H., H. Niu, H. Wang, W. Wang, X. Jin, H. Wang, H. Zhou, and T. Lin. 2021. Micro-meso porous structured carbon nanofibers with ultra-high surface area and large supercapacitor electrode capacitance. *Journal of Power Sources* 482 (August 2020):228986. doi:10.1016/j.jpowsour.2020.228986.
- Wang, A., K. Sun, R. Xu, Y. Sun, and J. Jiang. 2021. Cleanly synthesizing rotten potato-based activated carbon for supercapacitor by self-catalytic activation. *Journal of Cleaner Production* 283:125385. doi:10.1016/j.jclepro.2020.125385.
- Wang, J., X. Zhang, Z. Li, Y. Ma, and L. Ma. 2020. Recent progress of biomass-derived carbon materials for supercapacitors. *Journal of Power Sources* 451 (October 2019):227794. doi:10.1016/j.jpowsour.2020.227794.
- Wan, L., W. Wei, M. Xie, Y. Zhang, X. Li, R. Xiao, J. Chen, and C. Du. 2019. Nitrogen, sulfur co-doped hierarchically porous carbon from rape pollen as high-performance supercapacitor electrode. *Electrochimica acta* 311:72–82. doi:10.1016/j.electacta.2019.04.106.

- Wei, B., T. Wei, C. Xie, K. Li, and F. Hang. 2021. Promising activated carbon derived from sugarcane tip as electrode material for high-performance supercapacitors. *RSC advances* 11 (45):28138–47. doi:10.1039/d1ra04143f.
- Wickramaarachchi, W. A. M. K. P., M. Minakshi, X. Gao, R. Dabare, and K. W. Wong. 2021. Hierarchical porous carbon from mango seed husk for electro-chemical energy storage. *Chemical Engineering Journal Advances* 8:100158. doi:10.1016/j.ceja.2021.100158.
- Wu, L., Y. Cai, S. Wang, and Z. Li. 2021. Doping of nitrogen into biomass-derived porous carbon with large surface area using N<sub>2</sub> non-thermal plasma technique for high-performance supercapacitor. *International Journal of Hydrogen Energy* 46 (2):2432–44. doi:10.1016/j.ijhydene.2020.10.037.
- Zhang, P., W. Wang, Z. Kou, B. Wang, and X. Zhong. 2021. Low-cost and advanced symmetry supercapacitors based on three-dimensional tea waste of porous carbon nanosheets. *Materials Technology* 36 (1):1–10. doi:10.1080/10667857.2020.1714902.
- Zhang, Y., C. Wu, S. Dai, L. Liu, H. Zhang, W. Shen, W. Sun, and C. Ming Li. 2022. Rationally tuning ratio of micro- to meso-pores of biomass-derived ultrathin carbon sheets toward supercapacitors with high energy and high power density. *Journal of Colloid and Interface Science* 606:817–25. doi:10.1016/j.jcis.2021.08.042.
- Zhang, L., L. Xu, Y. Zhang, X. Zhou, L. Zhang, A. Yasin, L. Wang, and K. Zhi. 2018. Facile synthesis of bio-based nitrogen- and oxygen-doped porous carbon derived from cotton for supercapacitors. *RSC advances* 8 (7):3869–77. doi:10.1039/c7ra11475c.
- Zhou, X., P. Wang, Y. Zhang, L. Wang, L. Zhang, L. Zhang, L. Xu, and L. Liu. 2017. Biomass based nitrogen-doped structure-tunable versatile porous carbon materials. *Journal of Materials Chemistry A* 5 (25):12958–68. doi:10.1039/c7ta02113e.

# Sustainable development of biomass-derived activated carbon through chemical and physical activations and its effect on the physicochemical and electrochemical activity

## ORIGINALITY REPORT

14%

SIMILARITY INDEX

7%

INTERNET SOURCES

13%

PUBLICATIONS

1%

STUDENT PAPERS

## PRIMARY SOURCES

- 1 Chunhua Zhao, Yixuan Wang, Jiexin Zheng, Sijia Xu, Pengfei Rui, Chongjun Zhao. "Improved supercapacitor performance of  $\alpha$ -starch-derived porous carbon through gelatinization", Journal of Power Sources, 2022  
Publication 1%
- 2 Erman Taer, Nursyafni Syamsunar, Apriwandi Apriwandi, Rika Taslim. "Novel Solanum torvum Fruit Biomass-Derived Hierarchical Porous Carbon Nanosphere as Excellent Electrode Material for Enhanced Symmetric Supercapacitor Performance", JOM, 2023  
Publication <1%
- 3 [www.electrochemsci.org](http://www.electrochemsci.org)  
Internet Source <1%
- 4 Submitted to Universitas Riau  
Student Paper <1%
- 5 [dro.dur.ac.uk](http://dro.dur.ac.uk)  
Internet Source <1%

6	<a href="http://www.tandfonline.com">www.tandfonline.com</a> Internet Source	<1 %
7	<a href="http://www.nims.go.jp">www.nims.go.jp</a> Internet Source	<1 %
8	Moses Kigozi, Ravi Kali, Abdulhakeem Bello, Balaji Padya et al. "Modified Activation Process for Supercapacitor Electrode Materials from African Maize Cob", Materials, 2020 Publication	<1 %
9	<a href="http://iopscience.iop.org">iopscience.iop.org</a> Internet Source	<1 %
10	<a href="http://link.springer.com">link.springer.com</a> Internet Source	<1 %
11	John H. Lange, Kenneth W. Thomulka. "An evaluation of personal airborne asbestos exposure measurements during abatement of dry wall and floor tile/mastic", International Journal of Environmental Health Research, 3/1/2000 Publication	<1 %
12	<a href="http://ppid.unri.ac.id">ppid.unri.ac.id</a> Internet Source	<1 %
13	<a href="http://repository.ubaya.ac.id">repository.ubaya.ac.id</a> Internet Source	<1 %
14	Submitted to Chonnam National University Student Paper	<1 %



15

Juhan Lee, Soumyadip Choudhury, Daniel Weingarh, Daekyu Kim, Volker Presser. "High Performance Hybrid Energy Storage with Potassium Ferricyanide Redox Electrolyte", ACS Applied Materials & Interfaces, 2016

Publication

&lt;1 %

16

Samia Amara, Warda Zaidi, Laure Timperman, Georgios Nikiforidis, Mérièm Anouti. "Amide-based deep eutectic solvents containing LiFSI and NaFSI salts as superionic electrolytes for supercapacitor applications", The Journal of Chemical Physics, 2021

Publication

&lt;1 %

17

Shirley Palisoc, Joshua Marco Dungo, Michelle Natividad. "Low-cost supercapacitor based on multi-walled carbon nanotubes and activated carbon derived from Moringa Oleifera fruit shells", Heliyon, 2020

Publication

&lt;1 %

18

Zhaobing Fu, Kai Sun, Huailin Fan, Chao Li, Hong Liu, Shu Zhang, Kuan Ding, Guanggang Gao, Xun Hu. "Understanding evolution of the products and emissions during chemical activation of furfural residue with varied potassium salts", Journal of Cleaner Production, 2022

Publication

&lt;1 %

19

[xxtcl.sxicc.ac.cn](http://xxtcl.sxicc.ac.cn)

Internet Source

&lt;1 %

20

Hennen, William J., H. Marcel Sweers, Yi Fong Wang, and Chi Huey Wong. "Enzymes in carbohydrate synthesis. Lipase-catalyzed selective acylation and deacylation of furanose and pyranose derivatives", *The Journal of Organic Chemistry*, 1988.

Publication

&lt;1 %

21

Mingjiang Zhong, Eun Kyung Kim, John P. McGann, Sang-Eun Chun et al. "Electrochemically Active Nitrogen-Enriched Nanocarbons with Well-Defined Morphology Synthesized by Pyrolysis of Self-Assembled Block Copolymer", *Journal of the American Chemical Society*, 2012

Publication

&lt;1 %

22

[123docz.net](http://123docz.net)

Internet Source

&lt;1 %

23

Senthilkumar, S. T., R. Kalai Selvan, Y. S. Lee, and J. S. Melo. "Electric double layer capacitor and its improved specific capacitance using redox additive electrolyte", *Journal of Materials Chemistry A*, 2013.

Publication

&lt;1 %

24

Lingyan Zhu, Qifan Wang, Haotian Wang, Fei Zhao, Dongbing Li. "One-step chemical activation facilitates synthesis of activated

&lt;1 %

carbons from Acer truncatum seed shells  
for premium capacitor electrodes",  
Industrial Crops and Products, 2022

Publication

---

- 25 Rakhmawati Farma, Ade Nur Indah Lestari, Irma Apriyani. "Supercapacitor Cell Electrodes Derived from Nipah Fruticans Fruit Coir Biomass for Energy Storage Applications using Acidic and Basic Electrolytes", Journal of Physics: Conference Series, 2021

Publication

---

- 26 Sujata Mandal, Jiyao Hu, Sheldon Q. Shi. "A comprehensive review of hybrid supercapacitor from transition metal and industrial crop based activated carbon for energy storage applications", Materials Today Communications, 2023

Publication

---

- 27 Thanh-Tung Mai, Duc-Luong Vu, Dang-Chinh Huynh, Nae-Li Wu, Anh-Tuan Le. "Cost-effective porous carbon materials synthesized by carbonizing rice husk and K<sub>2</sub>CO<sub>3</sub> activation and their application for lithium-sulfur batteries", Journal of Science: Advanced Materials and Devices, 2019

Publication

---

- 28 Vinay S. Bhat, Titilope John Jayeoye, Thitima Rujiralai, Uraivan Sirimahachai, Kwok Feng Chong, Gurumurthy Hegde. "Acacia

auriculiformis–Derived Bimodal Porous Nanocarbons via Self-Activation for High-Performance Supercapacitors", *Frontiers in Energy Research*, 2021

Publication

29

[journals.tubitak.gov.tr](https://journals.tubitak.gov.tr)

Internet Source

<1 %

30

Awitdrus, Decha Apriliany Suwandi, Agustino, Erman Taer, Rakhmawati Farma, Romi Fadli Syahputra. "Effect of Aqueous Electrolyte to the Supercapacitor Electrode Performance Made from Sugar Palm Fronds Waste", *Journal of Physics: Conference Series*, 2021

Publication

<1 %

31

Chenjun He, Mei Huang, Li Zhao, Yongjia Lei, Jinsong He, Dong Tian, Yongmei Zeng, Fei Shen, Jianmei Zou. "Enhanced electrochemical performance of porous carbon from wheat straw as remolded by hydrothermal processing", *Science of The Total Environment*, 2022

Publication

<1 %

32

Rakhmawati Farma, Syarifah Famela Maurani, Irma Apriyani, Awitdrus, Yanuar, Ari Sulisty Rini. "Fabrication of Carbon Electrodes from Sago Midrib Biomass with Chemical Variation for Supercapacitor Cell Application", *Journal of Physics: Conference Series*, 2021

<1 %

33 Wu, N.L.. "Nanocrystalline oxide supercapacitors", *Materials Chemistry & Physics*, 20020428 <1 %  
Publication

---

34 Yair Korenblit, Marcus Rose, Emanuel Kockrick, Lars Borchardt, Alexander Kvit, Stefan Kaskel, Gleb Yushin. "High-Rate Electrochemical Capacitors Based on Ordered Mesoporous Silicon Carbide-Derived Carbon", *ACS Nano*, 2010 <1 %  
Publication

---

35 [arxiv.org](https://arxiv.org) <1 %  
Internet Source

---

36 [www.mdpi.com](https://www.mdpi.com) <1 %  
Internet Source

---

37 Damilola Momodu, Ndeye Fatou Sylla, Bridget Mutuma, Abdulhakeem Bello et al. "Stable ionic-liquid-based symmetric supercapacitors from Capsicum seed-porous carbons", *Journal of Electroanalytical Chemistry*, 2019 <1 %  
Publication

---

38 Submitted to Indian Institute of Technology, Kharagpure <1 %  
Student Paper

---

39 Jee Y. Hwang, Mengping Li, Maher F. El-Kady, Richard B. Kaner. "Next-Generation Activated Carbon Supercapacitors: A Simple <1 %

## Step in Electrode Processing Leads to Remarkable Gains in Energy Density", Advanced Functional Materials, 2017

Publication

---

40

Lu Luo, Lingcong Luo, Jianping Deng, Tingting Chen, Guanben Du, Mizi Fan, Weigang Zhao. "High performance supercapacitor electrodes based on B/N Co-doped biomass porous carbon materials by KOH activation and hydrothermal treatment", International Journal of Hydrogen Energy, 2021

Publication

---

<1 %

41

Mu, Xuemei, Yaxiong Zhang, Huan Wang, Baoyu Huang, Pengbo Sun, Tao Chen, Jinyuan Zhou, Erqing Xie, and Zhenxing Zhang. "A high energy density asymmetric supercapacitor from ultrathin manganese molybdate nanosheets", Electrochimica Acta, 2016.

Publication

---

<1 %

42

Raji Atchudan, Kanagesan Samikannu, Suguna Perumal, Thomas Nesakumar Jebakumar Immanuel Edison, Rajangam Vinodh, Yong Rok Lee. "Aesculus turbinata biomass-originated nanoporous carbon for energy storage applications", Materials Letters, 2021

Publication

---

<1 %

43

Ricardo Antonio Mendoza, Vicente Rodríguez-González, Anvar A Zakhidov, Stanislav Cherepanov, Arturo I Martinez, Jorge Oliva. "Using a mixture of vinasse-contaminant+H3PO4 as efficient electrolyte for high performance flexible carbon nanotube-based supercapacitors", Journal of Physics D: Applied Physics, 2021

Publication

&lt;1 %

44

Sivagaami Sundari Gunasekaran, Sushmee Badhulika. "Effect of pH and activation on macroporous carbon derived from cocoa-pods for high performance aqueous supercapacitor application", Materials Chemistry and Physics, 2022

Publication

&lt;1 %

45

Xiaodong Yang, Lili Wang, Xueqin Shao, Jin Tong, Rui Chen, Qiang Yang, Xizhen Yang, Guodong Li, Andrew R. Zimmerman, Bin Gao. "Preparation of biosorbent for the removal of organic dyes from aqueous solution via one-step alkaline ball milling of hickory wood", Bioresource Technology, 2022

Publication

&lt;1 %

46

[academic.ncl.res.in](http://academic.ncl.res.in)

Internet Source

&lt;1 %

47

[pure.ulster.ac.uk](http://pure.ulster.ac.uk)

Internet Source

&lt;1 %

48

E Taer, E Padang, N Yanti, Apriwandi, R Taslim. "Etlingera elatior leaf agricultural waste as activated carbon monolith for supercapacitor electrodes", Journal of Physics: Conference Series, 2021

Publication

&lt;1 %

49

Erman Taer, Apriwandi Apriwandi, Sielvya Chow, Rika Taslim. "Integrated pyrolysis approach of self-O-doped hierarchical porous carbon from yellow mangosteen fruit for excellent solid-state supercapacitor volumetric performance", Diamond and Related Materials, 2023

Publication

&lt;1 %

50

M. Karnan, K. Hari Prakash, Sushmee Badhulika. "Revealing the super capacitive performance of N-doped hierarchical porous activated carbon in aqueous, ionic liquid, and redox additive electrolytes", Journal of Energy Storage, 2022

Publication

&lt;1 %

51

Na Sun, Zeyang Li, Xian Zhang, Wenxiu Qin et al. "Hierarchical Porous Carbon Materials Derived from Kelp for Superior Capacitive Applications", ACS Sustainable Chemistry & Engineering, 2019

Publication

&lt;1 %

52

Shrabani De, Sourav Acharya, Sumanta Sahoo, Ganesh Chandra Nayak. "Present status of biomass-derived carbon-based

&lt;1 %



composites for supercapacitor application", Elsevier BV, 2020

Publication

---

53

Sivagaami Sundari Gunasekaran, Sushmee Badhulika. "'One-for-two' strategy of N-doped carbon as anode and ZnCo<sub>2</sub>O<sub>4</sub>/N-doped carbon nanocomposite as cathode for high-performance asymmetric supercapacitor application", New Journal of Chemistry, 2021

Publication

---

<1 %

54

Xiaohui Zhang, Zhian Qiu, Qingyu Li, Libo Liang, Xiaofei Yang, Shaorong Lu, Dinghan Xiang, Feiyan Lai. "Nickel Acetate-Assisted Graphitization of Porous Activated Carbon at Low Temperature for Supercapacitors With High Performances", Frontiers in Chemistry, 2022

Publication

---

<1 %

55

Zhanglin Liu, Jinguang Hu, Fei Shen, Dong Tian, Mei Huang, Jinsong He, Jianmei Zou, Li Zhao, Yongmei Zeng. "Trichoderma bridges waste biomass and ultra-high specific surface area carbon to achieve a high-performance supercapacitor", Journal of Power Sources, 2021

Publication

---

<1 %

Exclude bibliography  On